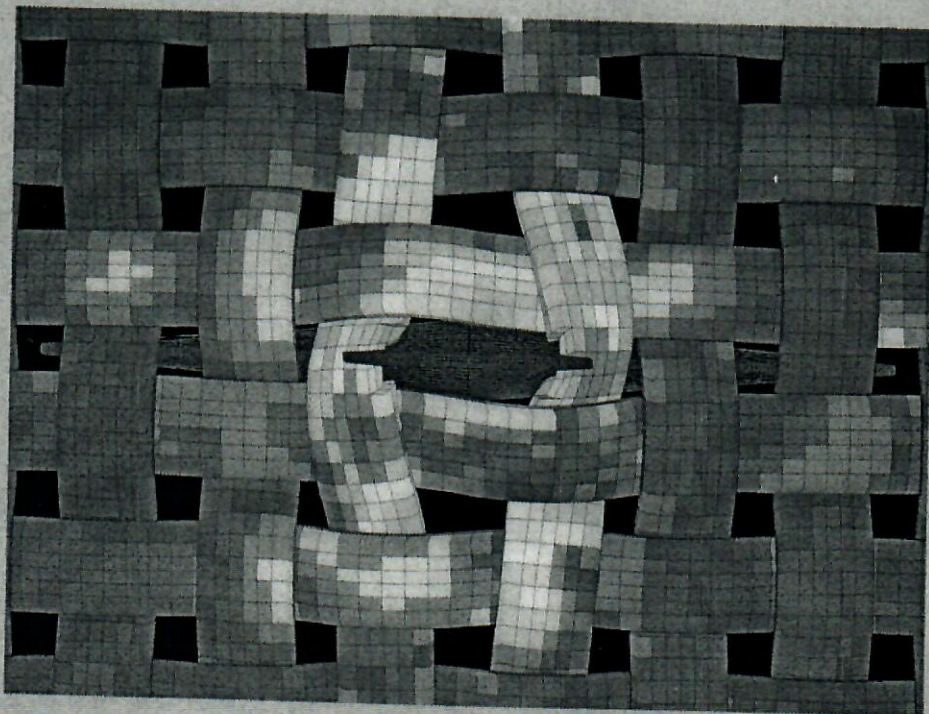# Proceedings of the Eighth International Conference on Computational Structures Technology

Edited by
B.H.V. Topping, G. Montero and R. Montenegro

Las Palmas de Gran Canaria - Spain
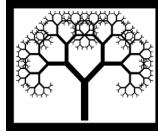12-15 September 2006

CIVIL-COMP PRESS

Cover Image: Yarn failure and element stress distributions during simulation of knife penetration into a woven fabric. This image is used with the permission of W.M. Gao. For more details, see Paper 90.

Contents

Modelling and Analysis of PVDF Copolymer-Ceramic Composite Thin Films

D.R. Mahapatra and R.V.N. Melnik
Mathematical Modelling and Computational Sciences
Wilfrid Laurier University, Waterloo, ON, Canada

Abstract

A mesoscopic model to analyze various effects of electroactive and flow related properties in piezoelectric copolymer composite thin film has been developed in this paper. A three-phase composite with piezoelectric particulate phase , electroactive polymer phase and graft polymer-matrix phase is considered. The homogenized constitutive model takes into account the local transport of cations in polymer, electrostriction and anhysteretic polarization. A finite strain description is given which includes the mesoscopic dispersion of copolymer chains. Finite element simulation is carried out by considering a P(VDF-TrFE)-PZT-Araldite thin film. Analysis of the results indicate that an increasing copolymer content substantially changes the deformation pattern in the film.

Keywords: piezoelectric, polymer, mesoscopic, finite strain, thin film.

1 Introduction

Polymer semiconductors and their composite variants with significant piezoelectric effect are considered as promising candidates to compete with the silicon based technology. Piezoelectric copolymer composite films, such as ultra-thin Langmuir-Boldgett films of PVDF and its copolymer with trifluoroethylene (P(VDF-TrFE)) [1], ionic polymer [4] and electrostrictive elastomers [11] have several potential applications, especially in photonics, bio-medical devices, macromolecular assembly and smart structures. The category of polymer composite we are interested in this paper is the one in which the piezoelectricity, the electrical charge and the polymer dispersion interplay to produce a desired functionality. Detailed discussions on the merits and demerits of various piezoelectric copolymer composites can be found in published literature (see references [2, 3, 4]). Computational models have been developed in literature for

1

polymer chains in solvent as they are solidified (see reference [7]). Substantial efforts have been devoted to the analysis of the equilibrium conformations of the polymer chains and their interactions in a non-Newtonian fluid. In the solid state, the dynamics of the piezoelectric copolymer (thin film) is governed by the deformation of the polymer chains which also undergo electrical polarization and transport of charge. Due to this coupled dynamics, the charge transport with dynamical changes in the conduction band of the polymeric network is of importance in photonics related applications. On the other hand, electrostriction induced mechanical motion and flexibility of the piezoelectric copolymer film is of importance for smart structural applications. Molecular level modeling of the dynamics and related observations have been reported in literature [9, 10]. Macroscopic effect of linear piezoelectricity and electrostriction in piezoelectric composite structures have been studied widely. However, in polymer composite, various effects which are important for small scale applications (e.g. flexible thin film device) have not been well reported in literature. In this paper, we develop a mesoscopic model to study these effects .

The outline of the paper is the following. In Sec. 2 we derive a constitutive model of a three-phase composite with piezoelectric particulate, electroactive polymer and elastomeric matrix. In Sec. 3 we give a kinematic description of the composite including the dispersion of the copolymers. The dynamics aspect is discussed in Sec. 4. In Sec. 5 we perform numerical simulation of mechanical deformation by considering P(VDF-TrFE)-PZT-Araldite thin film.

2 Constitutive Model

Here, we first discuss a general formulation of the piezoelectric polymer composite thin film problem. Electrical excitation to the film is generally given by surface electrodes. From the microscopic viewpoint, the mechanism of electrical excitation by electrode is not well defined. This is due to the fact that electrode material remains in a diffused state with the polymeric system and there is a lack of crystalline surfaces. Therefore, at the microscopic scale, the interaction in three-dimensional. On the other hand, for device level analysis and design optimization, a thin film type geometry requires a reduced dimensional model. By a mesoscopic modeling approach, we reduce the problem complexity from a three-dimensional polymeric composite system by reducing the details of the polymer dispersion and by applying appropriate boundary condition for deformation and electromagnetic fields in the thin film limit. In order to derive the dynamics in this mesoscopic modeling approach, we first construct a three-dimensional constitutive model and homogenize corresponding to a quasi-three dimensional situation.

We define the Cartesian components of stress ($\boldsymbol{\sigma}$), strain ($\boldsymbol{\varepsilon}$), electric charge displacement ($\boldsymbol{D}$), electric field intensity ($\boldsymbol{E}$), magnetic flux ($\boldsymbol{B}$) and the magnetic field intensity ($\boldsymbol{H}$) in (x, y, z). Our objective is to construct a constitutive model of the form

$$\boldsymbol{\sigma} = \boldsymbol{c}\boldsymbol{\varepsilon} + \tau\boldsymbol{c}'\dot{\boldsymbol{\varepsilon}} - \tau\dot{\boldsymbol{\sigma}} - \boldsymbol{\sigma}(\boldsymbol{E})_p, \tag{1a}$$
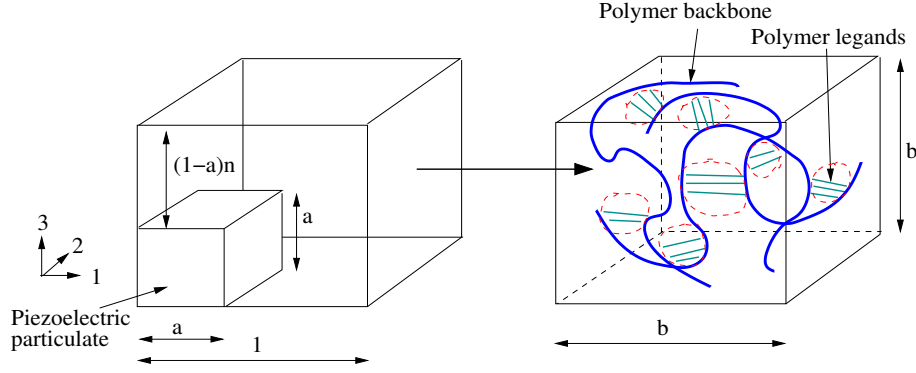
Figure 1: Schematic representation of the piezoelectric copolymer composition.

$$\boldsymbol{D} = \boldsymbol{\epsilon}\boldsymbol{E} + \boldsymbol{P}(\boldsymbol{\varepsilon}, \boldsymbol{E}), \tag{1b}$$

$$\boldsymbol{B} = \boldsymbol{\mu}\boldsymbol{H} + \mu_0\boldsymbol{M}(\boldsymbol{\varepsilon}), \tag{1c}$$

where $\boldsymbol{c}$ is the stiffness, $\boldsymbol{c}'$ is the flow coefficient, τ is a strain relaxation time constant, $\boldsymbol{\sigma}_p$ is the electric polarization induced stress, $\boldsymbol{\epsilon}$ is the dielectric permittivity, $\boldsymbol{P}$ is the electrical polarization vector due to transformation and deformation of the macro-molecular structure, $\boldsymbol{\mu}$ is the magnetic permeability and $\boldsymbol{M}$ is the magnetic polarization vector due to molecular spin. There can be several other effects depending on the composition of the piezoelectric polymer (e.g., inclusion of ferromagnetic particles, inclusions of left-handed material systems with negative index etc.), however increasing complexities in this way would restrict the use of experimentally measured material constants, since such experiments are performed on bulk sample without the effects of constraints on domain formation. The only straightforward yet computationally prohibitive method is then to perform molecular dynamic simulations. With the basic assumptions on the nature of the coupling among the mechanical and the electromagnetic field in Eqs. (1a)-(1c), we next consider individual structure of the linear and the nonlinear parts in the constitutive model.

We split the total charge density ρ_{total} and the total conduction current $\boldsymbol{J}_{\text{total}}$ as

$$\rho_{\text{total}} = \rho_c + \rho_p \quad \boldsymbol{J}_{\text{total}} = \boldsymbol{J} + \boldsymbol{J}_p + \boldsymbol{J}_{\text{m}}, \tag{2}$$

where ρ_c is the true charge density, ρ_p is the bound charge density, $\boldsymbol{J}$ is the true conduction current, $\boldsymbol{J}_p$ is the conduction current due to bound charge, $\boldsymbol{J}_m$ is the molecular current density. The local conservation laws are then

$$\nabla \cdot \boldsymbol{P} = -\rho_p, \quad \nabla \times \boldsymbol{M} = \boldsymbol{J}_m, \tag{3}$$

and the local continuity condition reads

$$\nabla \cdot \boldsymbol{J}_p = -\dot{\rho}_p. \tag{4}$$

ρ_c is related to the conduction current $\boldsymbol{J}$ by the continuity condition

$$\boldsymbol{\nabla} \cdot \boldsymbol{J} = -\dot{\rho}_c. \tag{5}$$

3

Eq. (5) has important to consider mainly for polymer semiconductor and chemically active electroactive polymers and gels. The bound charge density ρ_p is obtained from the molar concentration (c_n) of cations and the molar concentration (c_{group}) of charge groups in the polymer (e.g. sulfonic or carboxylic groups in ionic polymer composite [4]), which can be written as

$$\rho_p = (c_n - c_{\mathrm{group}})Ne \ , \tag{6}$$

where N is the Avogadro's number and e is the elementary charge of an electron. Further, the migration of cations can be important for certain polymers, which should then follow the Onsagar theory or irreversible thermodynamics. Neglecting the piezoelectric coupling in the constitutive model in Eqs. (1a)-(1c) for this local thermodynamics, one can write the ion transport equation as

$$\boldsymbol{J}_p = \sigma_c \boldsymbol{E} - \boldsymbol{L}\boldsymbol{\nabla}p \ , \tag{7}$$

and the solvent transport equation as

$$\boldsymbol{Q} = \boldsymbol{L}^T \boldsymbol{E} - K\boldsymbol{\nabla}p \ , \tag{8}$$

where $p = \frac{1}{3}\mathrm{Tr}(\boldsymbol{\sigma})$ is the hydrostatic stress, $\boldsymbol{Q}$ is the solvent flux, σ_c is the electric conductance, K is the Darcy permeability and $\boldsymbol{L}$ is a symmetric positive definite coefficient matrix obtained experimentally. Assuming that the solvent flux is negligible for solid-state applications, the local conservation equation due to migrating charge is expressed as

$$e\boldsymbol{E} \approx kT\boldsymbol{\nabla}(\ln(c_n)) \ , \tag{9}$$

where k is the Boltzman constant, T is the temperature. With the help of Eqs. (7) and (9) in Eq. (6), the continuity equation for the migrating charge finally becomes

$$\overline{\dot{(c_nN)}}e = \frac{\sigma_c}{e}kT\boldsymbol{\nabla}^2\left[\ln(c_n)\right] - \frac{1}{3}\boldsymbol{\nabla}\cdot\left(\boldsymbol{L}\boldsymbol{\nabla}\left[\mathrm{Tr}(\boldsymbol{\sigma})\right]\right) \ . \tag{10}$$

Further, for piezoelectric polymer blends, it is reasonable to adopt an averaging approach to obtain the true charge density and the effective dielectric properties. To this end, for the present study, we also neglect spin polarized current, i.e. $\boldsymbol{J}_m = 0$. Since in polymer blends, the poling can be done through network of metallic wires embedded in the solidified matrix phase, the conduction current induced charge density can have special distribution depending on the type of interaction between the the piezoelectric particles, the polymer-metal legands. The true charge density is assumed to be

$$\rho_c = \nu_{\mathrm{co}}(\rho_c)_{\mathrm{co}} + \nu_{\mathrm{pa}}(\rho_c)_{\mathrm{pa}} \ , \tag{11}$$

where ν_{co} and ν_{pa} are respectively the volume fraction corresponding to the copolymers and piezoelectric particles and they satisfy the relation

$$\nu_{\mathrm{co}} + \nu_{\mathrm{el}} = \frac{a + (1-a)n - a^2}{a + (1-a)n} \ , \quad \nu_{\mathrm{pa}} = \frac{a^2}{a + (1-a)n} \ . \tag{12}$$

With reference to Fig. 1, ν_{el} is the volume fraction of the elastomeric matrix. For piezoelectric composite thin film, it is convenient to consider the 0-3 connectivity. We employ the method of effective property calculation as reported by Banno and Saito [5], which is found to be effective for 0-3 composite with ellipsoidal inclusions. We write the effective dielectric constant as

$$\boldsymbol{\epsilon} = \boldsymbol{I}\epsilon , \quad \epsilon = \frac{a^2[a + (1-a)n]^2 \epsilon_1 \epsilon_{\mathrm{pa}}}{a\epsilon_{\mathrm{pa}} + (1-a)n\epsilon_1} + \{1 - a^2[1 + (1-a)n]\}\epsilon_{\mathrm{pa}} , \qquad (13)$$

where ϵ_1 is the effective dielectric constant for the copolymer-matrix, which is assumed to be

$$\epsilon_1 = \nu_{\mathrm{co}}\epsilon_{\mathrm{co}} + \nu_{\mathrm{el}}\epsilon_{\mathrm{el}} . \qquad (14)$$

ϵ_{pa}, ϵ_{co} and ϵ_{el} are the dielectric constants for the piezoelectric particulate, copolymer and matrix, respectively. The magnetic permeability is expressed as

$$\boldsymbol{\mu} = \boldsymbol{I}\mu , \quad \mu = \nu_{\mathrm{pa}}\mu_{\mathrm{pa}} + \nu_{\mathrm{co}}\mu_{\mathrm{co}} + \nu_{\mathrm{el}}\mu_{\mathrm{el}} , \qquad (15)$$

where μ_{pa}, μ_{co} and μ_{el} are magnetic permeability for the piezoelectric particulate, copolymer and matrix, respectively.

We now consider the calculation of effective stiffness, piezoelectric coupling and electrostriction. It should be noted that crystalinity may not exist for the polymer composite such as the three-phase system considered here. The constitutive behaviour can be anisotropic. However, for thin film type geometry, it is not practical to include the full anisotropy. Here we consider stiffness with monoclinic type for piezoelectric particulate, which is written as

$$\boldsymbol{c}_{\mathrm{pa}} = \begin{bmatrix} c_{11} & c_{12} & c_{13} & 0 & 0 & c_{16} \\ c_{12} & c_{22} & c_{23} & 0 & 0 & c_{26} \\ c_{13} & c_{23} & c_{33} & 0 & 0 & c_{36} \\ 0 & 0 & 0 & c_{44} & c_{45} & 0 \\ 0 & 0 & 0 & c_{54} & c_{55} & 0 \\ c_{16} & c_{26} & c_{36} & 0 & 0 & c_{66} \end{bmatrix} . \qquad (16)$$

The reference frame axes of the volume element are parallel to the global coordinate, where 3 indicates the direction normal to the film plane. The matrix phase is assumed to be isotropic with stiffness matrix denoted by $\boldsymbol{c}_{\mathrm{el}}$ in the coordinate system of the volume element. The polymer phase is modeled by one-dimensional chains with their orientation angle $\theta(x, y)$ of the backbone as shown in Fig. 2. The chain is extensible with small shear stiffness. The stiffness matrix for the chain in the coordinate system corresponding to the volume element is expressed as

$$\boldsymbol{c}_{\mathrm{co}} = \boldsymbol{\Gamma}(\theta)^T \boldsymbol{c}_{\mathrm{chain}} \boldsymbol{\Gamma}(\theta) , \qquad (17)$$

where $\boldsymbol{\Gamma}(\theta)$ is the transformation matrix for the symmetric fourth rank tensor. With the introduction of individual forms of the electrostriction and polarization, which is

discussed next, we perform averaging of the stiffness and the piezoelectric properties considering linear parts of the constitutive model. This is done by taking into account the 0-1, 0-2 average correction on the effective dielectric constant derived in Eq. (13). For analysis of the thin film, we use a plane-stress type approximation with the assumption of parallel electrode on the film surfaces.

The polarization induced stress in the constitutive model in Eq. (1a) is considered to be of the following form

$$\boldsymbol{\sigma}(\boldsymbol{E})_p = \boldsymbol{e}^T \boldsymbol{E} + \boldsymbol{c}Q\epsilon_0^2(\boldsymbol{\epsilon} - \boldsymbol{I})^2 \begin{bmatrix} 1 & 0 & 0 \\ 0 & 1 & 0 \\ 0 & 0 & 0 \end{bmatrix} E_z^2 + \epsilon_0^2\boldsymbol{\epsilon} \begin{bmatrix} 1 & 0 & 0 \\ 0 & 1 & 0 \\ 0 & 0 & 0 \end{bmatrix} E_z^2 \ , \quad (18)$$

where $\boldsymbol{e}$ is the effective piezoelectric coefficient matrix obtained by averaging of the three-phase linear model, Q is the electrostrictive coefficients. In Eq. (18), the second term describes the stress due to electrostriction and the third term describes the Maxwell stress. The polarization vector $\boldsymbol{P}$ is considered to be of the following form

$$\boldsymbol{P}(\boldsymbol{\varepsilon}, \boldsymbol{E}) = \boldsymbol{e}\boldsymbol{\varepsilon} + \boldsymbol{\Gamma}(\theta)'^T P_s \tanh\left(\frac{E_e}{a}\right) \boldsymbol{\Gamma}(\theta)' \ , \quad (19)$$

where the first term describes the electric displacement due to polarization of the predominantly piezoelectric particulate-matrix phase and the second term describes the anhysteretic polarization of the oriented polymer chain constrained by the piezoelectric particulate-matrix phase, which is based on Ising-spin relation [6]. Here $\boldsymbol{\gamma}(\theta)'$ is the vector transformation matrix, P_s is the saturation polarization, E_e is the effective electric field acting along the dipole moment and is expressed as

$$E_e = E_{||} + \alpha P_s \tanh\left(\frac{E_e}{a}\right) \ , \quad (20)$$

$\alpha = \hat{E}/P_s$ with $\hat{E}$ as the scaling electric field, and a is a constant given by $a = \hat{E}T/(3T_c$ where T_c is the Curie temperature of the composition. $\hat{E}$, a and α are to be estimated from experimental data. The parallel electric field $E_{||}$ is related to the components of the electric field vector in the film coordinate (see Fig. 2) as

$$E_{||} = \sqrt{E_x^2 + E_y^2} \ . \quad (21)$$

3   Mesoscopic Kinematics

Having defined various terms in the constitutive model, the main task is now to derive the kinematics of the three-phase composite at the mesoscopic scale. Here we first define the displacement field as

$$\boldsymbol{u} = \boldsymbol{u}_{\text{ep}} + \frac{1}{m}\sum_{i=1}^m \boldsymbol{v}_i \ , \quad (22)$$

6

where $\boldsymbol{u}_{\mathrm{ep}} = \{u_x\, u_y\, u_z\}^T$ denotes the displacement vector due elastic deformation of the predominantly piezoelectric particulate-matrix phase, m is the number of copolymer chains present in the volume element, $\boldsymbol{v}_i$ denotes displacement due to the kinematics of the segment of the chain with length $m'a_0$ centered at a material point i with coordinate (x_i, y_i), where m' is the number of blocks in the segment of the chain and a_0 is the C-C bond length in the backbone. The segment of the chain is assumed to be oriented at an angle $\theta_i = \theta$ as shown in Fig. 2(b). The kinematics of the segment can be described as

$$
\boldsymbol{v}_i = m'a_0 \left[1 - \cos\left(\theta(x_i, y_i)_i - \theta(x_i, y_i)_i^0\right)\right]
\left\{
\begin{array}{c}
\cos\theta(x_i, y_i)_i^0 \\
\sin\theta(x_i, y_i)_i^0 \\
0
\end{array}
\right\} ,
\tag{23}
$$

where $\theta(x_i, y_i)_i^0$ denotes the saturation conformation under the applied mechanical and electrical loading. In general, the flow in the copolymer phase in terms of its distribution $\boldsymbol{v}_i$ should follow a kinetic law (e.g. Smoluchowski equation of disperse collidal system [7]. However, solving the mesoscopic dynamics including this dispersion effect is not an easy task. Instead, in the present model we prescribe the distribution of the saturation conformation in terms of θ_i^0 and solve the equations of motion.

The finite strain $\boldsymbol{\varepsilon}$ is expressed as

$$
\boldsymbol{\varepsilon} = \frac{1}{2} \left[\boldsymbol{\nabla}\boldsymbol{u} + (\boldsymbol{\nabla}\boldsymbol{u})^T + (\boldsymbol{\nabla}\boldsymbol{u})^T\boldsymbol{\nabla}\boldsymbol{u}\right] .
\tag{24}
$$

With the help of Eq. (25) in Eq. (24) and neglecting the small order term, we arrive at the following form

$$
\boldsymbol{\varepsilon} \approx \frac{1}{2} \left[\boldsymbol{\nabla}\boldsymbol{u}_{\mathrm{ep}} + (\boldsymbol{\nabla}\boldsymbol{v})_{\mathrm{ep}}^T + \frac{1}{m}\sum_{i=1}^{m}\boldsymbol{\nabla}\boldsymbol{v}_i + \frac{1}{m}\sum_{i=1}^{m}(\boldsymbol{\nabla}\boldsymbol{v}_i)^T + \frac{1}{m}\left(\sum_{i=1}^{m}\boldsymbol{\nabla}\boldsymbol{v}_i\right)^T \boldsymbol{\nabla}\boldsymbol{u}_{\mathrm{ep}} \right.
$$

$$
\left. + \frac{1}{m}(\boldsymbol{\nabla}\boldsymbol{u}_{\mathrm{ep}})^T \left(\sum_{i=1}^{m}\boldsymbol{\nabla}\boldsymbol{v}_i\right) + \frac{1}{m^2}\left(\sum_{i=1}^{m}\boldsymbol{\nabla}\boldsymbol{v}_i\right)^T \left(\sum_{i=1}^{m}\boldsymbol{\nabla}\boldsymbol{v}_i\right) \right] .
\tag{25}
$$

4   Equations of Motion

The momentum conservation equation is expressed as by keeping the electrostriction induced terms on the right hand side as coupling term.

$$
\rho\frac{\partial^2 \boldsymbol{u}}{\partial t^2} - \boldsymbol{\nabla}\cdot\boldsymbol{\sigma} = \boldsymbol{0} ,
\tag{26}
$$

where the effective mass density $\bar{\rho}$ is given by

$$
\bar{\rho} = \nu_{\mathrm{el}}(\bar{\rho})_{\mathrm{el}} + \nu_{\mathrm{pa}}(\bar{\rho})_{\mathrm{pa}} + \nu_{\mathrm{co}}(\bar{\rho})_{\mathrm{co}} .
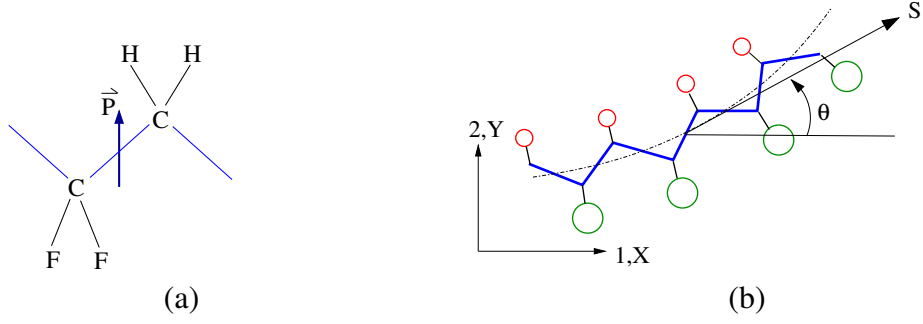\tag{27}
$$

Figure 2: (a) PVDF molecular structure with local polarization vector $\boldsymbol{P}$ (b) oriented polymer chain with angle θ in the thin film coordinate system XY.

We simplify the stress gradient terms arising in Eq. (26) using Eq. (1a) and move the terms due to piezoelectricity and electrostriction to the the right hand side. In this manner we seek the solution in the mechanical deformation with distributed electrical source. For example, the linear components on the right-hand electrical source term are written as

$$f_x = -e_{31}\frac{\partial E_z}{\partial x} - e_{36}\frac{\partial E_z}{\partial y} \; , \quad f_y = -e_{36}\frac{\partial E_z}{\partial x} - e_{32}\frac{\partial E_z}{\partial y} \; , \quad f_z = -e_{33}\frac{\partial E_z}{\partial y} \; . \quad (28)$$

Note that here f_x, f_y and f_z are a functions of the transverse electric field E_z only. This is due to the particular form of piezoelectric coupling and the electric field approximation for the thin film, i.e., $E_z = -\partial \Phi(x,y)/\partial z$ with $\Phi(x,y)$ as the applied voltage. This is a reasonably simple type of electromechanical coupling (apart from the nonlinear parts), yet an important one to analyze the in-plane deformation and shear bands

The electric field has to satisfy Maxwell equations which are expressed as

$$\nabla \times \boldsymbol{E} = -\dot{\boldsymbol{B}}, \tag{29}$$

$$\nabla \times \boldsymbol{H} = \dot{\boldsymbol{D}} + \sigma_c \boldsymbol{E} + \boldsymbol{J}_{\text{total}} \; , \tag{30}$$

$$\nabla \cdot \boldsymbol{D} = \rho_{\text{total}} \; , \tag{31}$$

$$\nabla \cdot \boldsymbol{B} = 0 \; , \tag{32}$$

where $\boldsymbol{B}$ is the magnetic induction given by $\boldsymbol{B} = \boldsymbol{muH}$. The associated general impedance boundary conditions are

$$\boldsymbol{n} \times (\boldsymbol{E} - \boldsymbol{E}_\perp) = -\boldsymbol{J}_{sm} \; , \quad \boldsymbol{n} \times (\boldsymbol{H} - \boldsymbol{H}_\parallel) = \boldsymbol{J}_s \tag{33}$$

at surfaces $z_\perp = -h/2, +h/2$, and

$$\boldsymbol{n} \cdot \boldsymbol{D} = \rho_s \; , \quad \boldsymbol{n} \cdot \boldsymbol{B} = 0 \tag{34}$$

at the surfaces. Here, ρ_s as the surface charge, $\boldsymbol{n}$ is the unit outward surface-normal.

8

By using the constitutive model derived in Sec. 2, Maxwell's equations in (29)-(32) are combined into the following system of coupled hyperbolic equations

$$\mu\epsilon\frac{\partial^2 \boldsymbol{E}}{\partial t^2}+\sigma_c\mu\frac{\partial \boldsymbol{E}}{\partial t}-\boldsymbol{\nabla}^2\boldsymbol{E}+=\boldsymbol{\epsilon}^{-1}\boldsymbol{\nabla}\rho_{\text{total}}+\mu\dot{\boldsymbol{J}}_{\text{total}}+\boldsymbol{\epsilon}^{-1}\boldsymbol{\nabla}\boldsymbol{\nabla}\cdot[\boldsymbol{P}(\boldsymbol{\varepsilon},\boldsymbol{E})]-\mu\frac{\partial^2}{\partial t^2}[\boldsymbol{P}(\boldsymbol{\varepsilon},\boldsymbol{E})]\ ,$$
(35)

$$\mu\epsilon\frac{\partial^2 \boldsymbol{H}}{\partial t^2}+\sigma_c\mu\frac{\partial \boldsymbol{H}}{\partial t}-\boldsymbol{\nabla}^2\boldsymbol{H}=-\boldsymbol{\nabla}\times\boldsymbol{J}_{\text{total}}+\boldsymbol{\nabla}\times\frac{\partial}{\partial t}[\boldsymbol{P}(\boldsymbol{\varepsilon},\boldsymbol{E})]\ .$$
(36)

Eqs. (35)-(36) can further be expressed in concise form, as

$$\mu\epsilon\frac{\partial^2 \boldsymbol{E}}{\partial t^2}+\sigma_c\mu\frac{\partial \boldsymbol{E}}{\partial t}-\boldsymbol{\nabla}^2\boldsymbol{E}=\boldsymbol{g}^E\ ,$$
(37)

$$\mu\epsilon\frac{\partial^2 \boldsymbol{H}}{\partial t^2}+\sigma_c\mu\frac{\partial \boldsymbol{H}}{\partial t}-\boldsymbol{\nabla}^2\boldsymbol{H}=\boldsymbol{g}^H\ ,$$
(38)

where the components of the right-hand-side represents the source terms due to deformation, hysteresis and charge transport, and they are coupled with Eq. (26). When the hysteresis and charge transport is absent, one could write

$$g^E_x=\epsilon_{11}^{-1}\frac{\partial^2 \bar{P}}{\partial x\partial z}\ ,\quad g^E_y=\epsilon_{22}^{-1}\frac{\partial^2 \bar{P}}{\partial y\partial z}\ ,\quad g^E_z=\epsilon_{33}^{-1}\frac{\partial^2 \bar{P}}{\partial^2 z}-\mu_{33}\frac{\partial^2 \bar{P}}{\partial t^2}\ ,$$
(39)

$$g^H_x=\frac{\partial^2 \bar{P}}{\partial y\partial t}\ ,\quad g^H_y=-\frac{\partial^2 \bar{P}}{\partial x\partial t}\ ,\quad g^H_z=0\ ,$$
(40)

and $\bar{P}$ is the effective polarization (a scalar quantity) due to piezoelectricity, which is given by

$$\bar{P}=e_{31}\varepsilon_{xx}+e_{32}\varepsilon_{yy}+e_{33}\varepsilon_{zz}+e_{36}\varepsilon_{xy}\ .$$
(41)

We solve the coupled system of hyperbolic equations (26), (37) and (38), supplemented by associated boundary conditions, in $\{\boldsymbol{u},\boldsymbol{E},\boldsymbol{H}\}$ by finite element discretization. Charge transport and kinetics of the flow have not been coupled with the present model. Due to the geometry $(x,y,z)\in[0,L_x]\times[0,L_y]\times[-h/2,h/2]$ and the thin film limit ($h\to 0$), we choose the following form of the electromagnetic field

$$\boldsymbol{E}=\left\{\begin{array}{c}E(x,y)_x\\[4pt]E(x,y)_y\\[4pt]-(z/h^2)\Phi(x,y)\end{array}\right\}\ ,\quad \boldsymbol{H}=\left\{\begin{array}{c}H(x,y)_x\\[4pt]H(x,y)_y\\[4pt]0\end{array}\right\}\ ,$$
(42)

where $\Phi(x,y)$ is the potential between the parallel surface electrodes. Distribution of the potential can be prescribed for electrical excitation and the system can be solved for $\boldsymbol{u}_{\text{ep}}$ and $\{E_x\,E_y\,H_x\,H_y\}$, whereas for mechanical actuation we solve the system for $\boldsymbol{u}_{\text{ep}}$ and $\{E_x\,E_y\,\Phi\,H_x\,H_y\}$.

5 Numerical Simulations

COMSOL multiphysics modelling software package [8] has been used for finite element simulation with right-hand side coupling terms in the governing partial differential differential equations. P(VDF-TrFE) copolymer blend with araldite is considered. PZT is considered as the piezoelectric particulate phase. A square film geometry of size $L_x = L_y = 0.05m$ and thickness $h = 2mm$ is discretized by tetrahedral Lagrangian finite element with second order accurate time stepping scheme. A deterministic distribution of chains angles θ has been used, which is given by

$$\theta(x_i, y_i)_i = \frac{\pi}{4} \left[\frac{x_i(L_x - x_i)}{L_x^2} + \frac{x_i(L_x - x_i)}{L_x^2} \right] \ , \quad \theta(x_i, y_i)_i^0 = 0 \ . \tag{43}$$

Material properties are used from the published literature (see [12, 2]). Effects of increase in the copolymer volume fraction on the deformation under mechanical loading are analyzed below. We apply a sinusoidal displacement of amplitude $2.5mm$ uniformly and normal to the parallel edges $x = 0, L_x$. Time period of the applied displacement history is taken as $T_u = 10s$. For the first sample we consider $\nu_{\text{co}} = 0.2$, $a = 0.8$, $n = 8.5$ which represents a predominantly piezoelectric composite film. Figs. 3(a) and (b) show the contours of longitudinal displacement u_1 and lateral displacement u_2, respectively, at $t = T_u/4$. Figs. 3(c) and (d) show the longitudinal strain ε_{xx} and the lateral strain ε_{yy} contours, respectively for the same composition. These figures reveal usual deformation patterns for the piezoelectric composite at the mesoscopic and macroscopic scales. Next we increase the copolymer volume fraction to $\nu_{\text{co}} = 0.5$ with $a = 0.5$, $n = 8.5$. Fig. 4(a) shows the u_1 contours at $t = T_u/8$ which indicates tensile load initiation. In this figure, a large pair of deformation gradients parallel to the loaded edges can be seen. Such deformation gradients were not observed for the composition with high piezoelectric particulate and low copolymer volume fraction. Figs. 4(b) and (c) show $u1$ and u_2 contours at $t = T_u/4$ which also indicate fully developed strain gradient zones. Comparing these two figures with Figs. 3(a) and (b) for the low copolymer high piezoelectric particulate composition, we observe that an increase in the copolymer volume fraction leads to specific shape of the strained region with high amount of flow, which is due to the stretching of the copolymer chains. From the Figs. 4(d) and (e) of strain contours, we can clearly observe the diagonally oriented patterns of principle strains. With these strained patterns we also see one order higher magnitude compared to the continuous patterns of the principle strains observed in case of low piezoelectric and high piezoelectric composition (see Figs. 3(c) and (d)).

6 Conclusions

A mesoscopic model to analyze various effects of electroactive and flow related properties in piezoelectric copolymer composite thin film has been developed in this paper. The three-phase constitutive model takes into account the local transport of cations for

ionic polymer, electrostriction and anhysteretic polarization within a simple constitutive averaging scheme. A finite strain description is given to model the kinematics of the copolymer chains. Finite element simulation is carried out by considering a P(VDF-TrFE)-PZT-Araldite thin film. Increasing copolymer content substantially changes the deformation pattern in the film.

References

[1] S. Palto, L. Blinov, A. Bune, E. Dubovik, V. Fridkin, N. Petukhova, K. Verkhovskaya, S. Yudin, *"Ferroelectric Langmuir-Blodgett films"*, Ferroelectric Lett., 19, 65, 1995.

[2] J.S. Harrison and Z. Ounaies, *"Piezoelectric Polymers"*, ICASE Report No. 2001-43, NASA/CR-2001-211422, 1-26, 2001.

[3] T. Furukawa, "Structure and functional properties of ferroelectric polymer", Advnac. Colloid and Interface Sci., 1997, 183-308, 1997.

[4] M. Shahinpoor, *"Inonic polymer-conductor composite as biomimetic sensors, robotic actuators and artificial muscles - a review"*, Electrochemica Acta, 48, 2343-2353, 2003.

[5] H. Banno and S. Saito, *"Piezoelectric and dielectric properties of composites of synthetic rubber and PbTiO$_3$ or PZT"*, J. Appl. Phys., 22(2), 67, 1983.

[6] R. C. Smith and C. L. Hom, *"A domain wall theory of ferroelectric hysteresis"*, J. Intelligent Mater. Sys. Struct., 10(3), 195-213, 1999.

[7] T. S. Chow, *"Mesoscopic Physics of Complex Materials"*, Springer-Verlag, NY, 2000.

[8] COMSOL, "Multiphysics User's Guide", COMSOL AB, Burlington, MA, 2005.

[9] J. D. Carbeck and G. C. Rutledge, *"Temperature dependent elastic, piezoelectric and pyroelectric properties of β-poly(vynylidene fluoride) from molecular simulation"*, Polymer, 37(22), 5089-5097, 1996.

[10] J. A. Young, B. L. Farmer and J. A. Hinkley, *"Molecular modeling of the poling of piezoelectric polyamides"*, Polymer, 40, 2787-2795, 1999.

[11] R. Pelrine, R. Kornbluh and J. Joseph, *"Electrostriction of polymer dielectrics with compliant electrodes as a means of actuation"*, Sensors and Actuators A: Phys., 64, 77-85, 1999.

[12] T.E. Gomez and F.M. Espinosa and F. Levassort and M. Lethiecq and A. James and E. Ringgard and C. E. Millar and P. Hawkins, *"Ceramic powder-polymer piezocomposites for electroacoustic transduction: modeling and design"*, Ultrasonics, 36, 907-923, 1998.
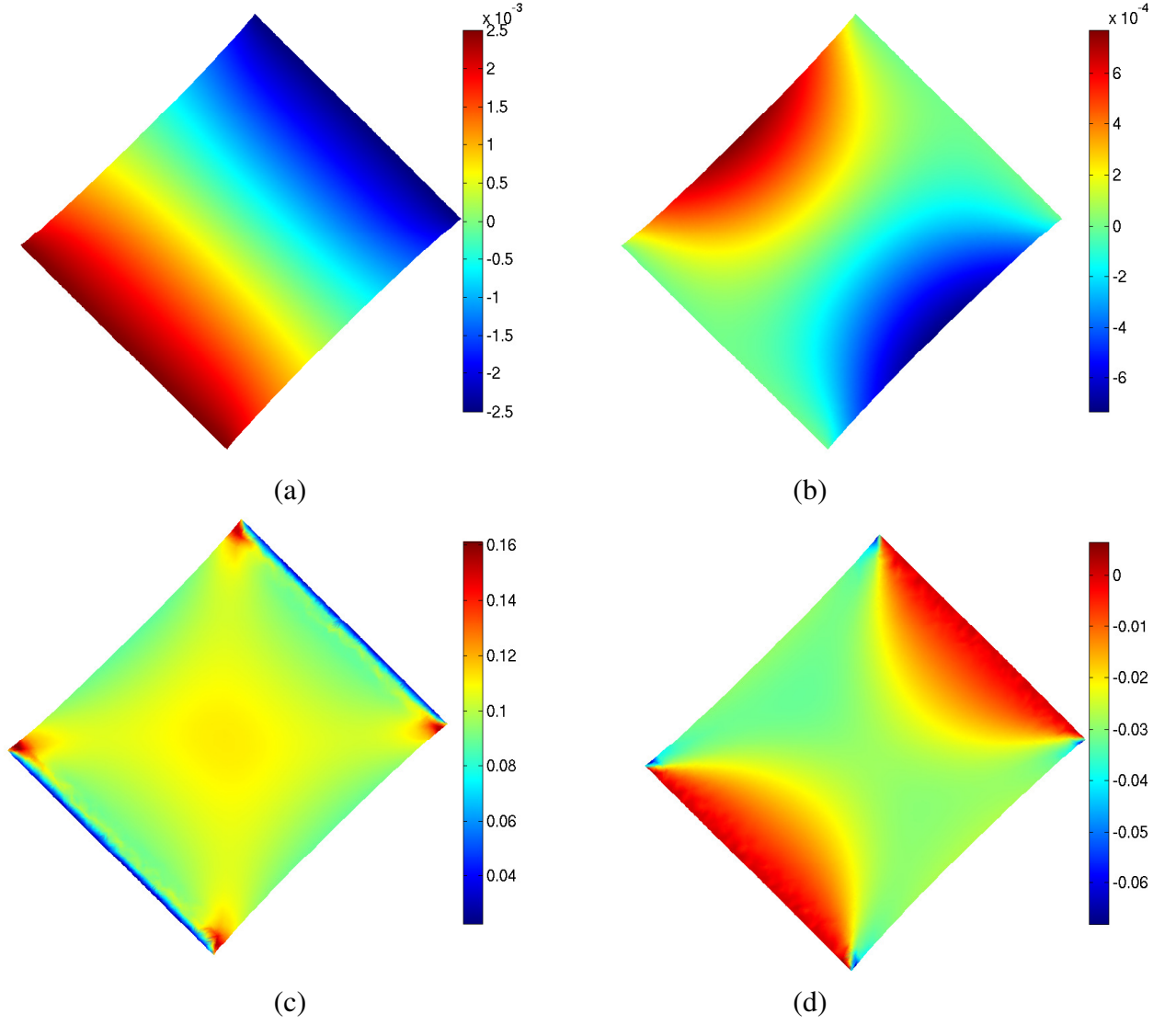
Figure 3: (a) Longitudinal displacement u_1 (b) lateral displacement u_2 (c) longitudinal strain ε_{xx} and (d) and lateral strain ε_{yy} contours at $t = T_u/4$. Volume fraction of copolymer is 0.2, $a = 0.8$.
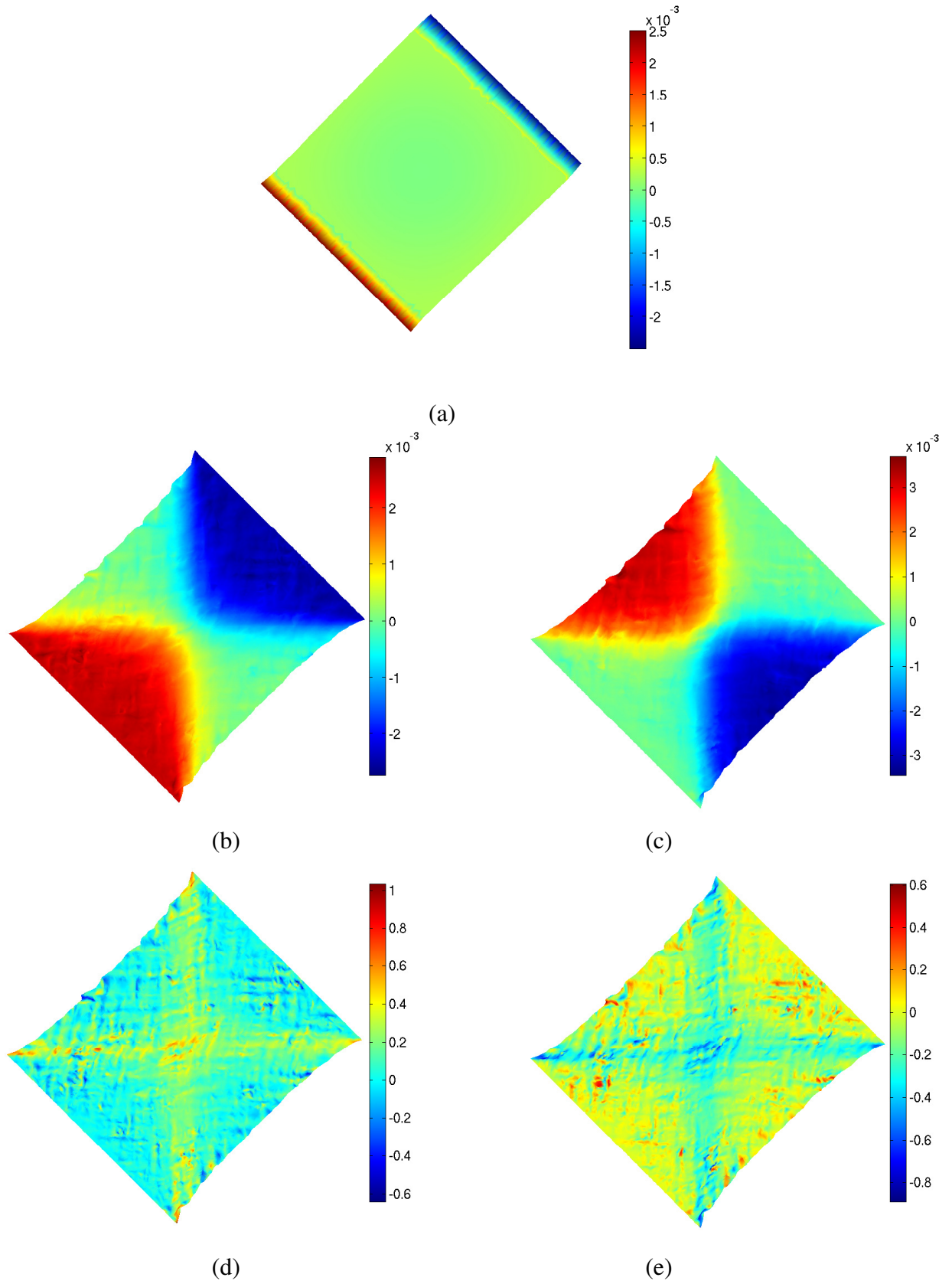
Figure 4: (a)Longitudinal displacement u_1 contour at $t = T_u/8$. Longitudinal displacement u_1 (b) lateral displacement u_2 (c) longitudinal strain ε_{xx} and (d) and lateral strain ε_{yy} contours at $t = T_u/4$. Volume fraction of copolymer is 0.5, $a = 0.5$.

Proceedings of the Eighth International Conference on Computational Structures Technology

Edited by B.H.V. Topping, G. Montero and R. Montenegro

This book contains the extended abstracts of the contributed papers presented at the Eighth International Conference on Computational Structures Technology, held in Las Palmas de Gran Canaria, Spain, 12-15 September 2006.

The full length papers are available in electronic format on the accompanying CD-ROM. The topics covered include:

- Damage, Robustness & Service-Life
- Steel and Composite Structures
- Probabilistic Approaches
- Tall Buildings
- Dynamics & Traffic Vibrations
- Constitutive & Material Modelling
- Viscoelastically Damped Structures
- Masonry Structures
- Fabric, Cable & Membrane Structures
- Composite & Adaptive Structures
- Steel Structures
- Reinforced Concrete Structures
- Aluminium Structures
- Structural Analysis & Re-Analysis

- Bridge Engineering
- Joints & Connections
- Plates & Shells
- FEM, DEM & BEM
- Iterative Solution Methods
- Meshless Methods
- Multiscale Methods
- Adaptivity & Errors
- Buckling & Post-Buckling
- Optimization
- Design Methods & Studies
- Seismic Engineering
- Composite Materials
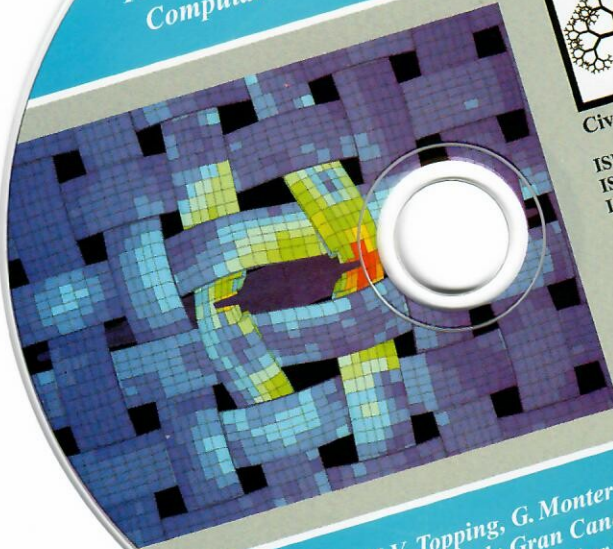- Piezoelectric Materials

A keyword and author index is provided both in this book and on the CD-ROM.

Proceedings of
The Eighth International Conference on
Computational Structures Technology

Civil-Comp Press

ISBN 1-905088-06-X Book
ISBN 1-905088-07-8 CD-ROM
ISBN 1-905088-08-6 Set

COMPACT
disc
DATA STORAGE

Edited by B.H.V. Topping, G. Montero and R. Montenegro
Las Palmas de Gran Canaria - Spain
12-15 September 2006